Biogeosciences Discuss., https://doi.org/10.5194/bg-2018-51
Manuscript under review for journal Biogeosciences
Discussion started: 1 February 2018

Biogeosciences Discussions Open Access EGU

Riverine carbon export in the arid-semiarid Wuding River catchment on the Chinese Loess Plateau

Lishan Ran[1], Mingyang Tian[2], Nufang Fang[3], Suiji Wang[4], Xixi Lu[2,5], Xiankun Yang[6], Frankie Cho[1]

[1]Department of Geography, The University of Hong Kong, Pokfulam Road, Hong Kong
[2]School of Ecology and Environment, Inner Mongolia University, Hohhot, China
[3]State Key Laboratory of Soil Erosion and Dryland Farming on the Loess Plateau, Institute of Soil and Water Conservation, Northwest A&F University, Yangling, China
[4]Institute of Geographical Sciences and Natural Resources Research, Chinese Academy of Sciences, Beijing, China
[5]Department of Geography, National University of Singapore, Singapore
[6]School of Geographical Sciences, Guangzhou University, Guangzhou, China

Abstract: Riverine export of terrestrially-derived carbon represent a key component of the global carbon cycle. In this study we quantify the redistribution of riverine carbon within the Wuding catchment on the Chinese Loess Plateau. Export of dissolved organic and inorganic carbon (DOC and DIC) exhibited pronounced spatial and temporal variability. While the DOC concentration was spatially comparable within the catchment, it was generally higher in spring and summer than in autumn, especially in the loess subcatchment. This reflects the enhanced organic matter inputs from agricultural tillage in spring and from terrestrial ecosystems in summer. DIC concentration in the loess subcatchment is significantly higher than that in the sandy subcatchment, due largely to dissolution of carbonates that are abundant in loess. In addition, content of particulate organic carbon (POC) shown strong seasonal variability with low values in the wet season owing to input of subsurface soils by gully erosion. The downstream carbon flux was $(7\pm1.9)\times10^{10}$ g C year^{-1} and dominated by DIC and POC. Total CO_2 emissions from water surface were $(3.7\pm0.5)\times10^{10}$ g C year^{-1}. Radiocarbon analysis revealed that the degassed CO_2 was 810–1890 years old, indicating the release of old carbon previously stored in soil horizons. Riverine carbon export in the Wuding catchment has been greatly modified by check dams. Our estimate shows that carbon burial through sediment storage was $(7.8\pm4.1)\times10^{10}$ g C year^{-1}, representing 42% of the total riverine carbon export from terrestrial ecosystems on an annual basis ($(18.5\pm4.5)\times10^{10}$ g C year^{-1}). Moreover, the riverine carbon export accounted for 16% of the catchment NEP. It appears that the magnitude of carbon sink of terrestrial ecosystems in this arid-semiarid catchment has been significantly offset by riverine carbon export.

1. Introduction

Inland waters (e.g., rivers, lakes, and dam-formed reservoirs) are a key component of the global carbon cycle (Cole et al., 2007;Regnier et al., 2013). Of these water bodies, rivers play an exceptionally significant role by directly linking terrestrial ecosystems and the oceans. Prior studies indicate that the amount of terrestrially-derived carbon entering inland waters was substantially larger than that discharged into the oceans mainly through fluvial transport of global rivers (Mendonça et al., 2017;Battin et al., 2009). With respect to river systems, this carbon imbalance suggests that rivers are not passive pipes simply transporting terrestrial carbon,

but are biogeochemically active in processing massive quantities of carbon along river course. Riverine carbon is subject to a number of physical and biogeochemical processes, such as burial, evasion, in-situ production, and decomposition. The CO_2 emissions from water surface of global rivers and streams combined are conservatively estimated at 1.8 Pg C $year^{-1}$ (Raymond et al., 2013). In addition, carbon loss due to long-term sediment storage in reservoirs through burial is also substantial (Battin et al., 2009;Cole et al., 2007;Mendonça et al., 2017;Clow et al., 2015). Inclusion of CO_2 emissions and carbon burial in sediments is thus critical for a holistic understanding of carbon cycling in river systems at different spatial scales.

Although studies on riverine fluxes of carbon have been exponentially increasing over the recent 20 years, great uncertainties remain to be properly resolved even for catchment-scale assessments, not to mention the larger regional and global estimates (Marx et al., 2017). An important source for these uncertainties is the underrepresentation of current carbon flux measurements, which are mostly confined to tropical and boreal rivers that are sensitive to climate change. In contrast, few studies have investigated the terrestrial and fluvial fluxes of carbon in arid and semiarid rivers though they are globally abundant (Tranvik et al., 2009). Increased concerns over global riverine carbon export and emissions necessitate an improved understanding of carbon cycling in these underexplored rivers. Studying their riverine carbon cycling on the basis of individual catchments will shed light on refining global riverine carbon flux estimates and thereby assessing their biogeochemical importance, as has been done for tropical and temperate rivers (e.g., Butman and Raymond, 2011; Richey et al., 2002).

With the role of arid-semiarid rivers in global riverine carbon cycle in mind, we investigated the transport and fate of carbon from terrestrial ecosystems through drainage network to catchment outlet in the medium-sized Wuding catchment on the arid-semiarid Loess Plateau (in northern China). The overall aim of this study was to quantify the redistribution of riverine carbon among its three pathways, including downstream export to catchment outlet, CO_2 evasion from water surface, and organic carbon (OC) burial through sediment storage, within the arid-semiarid Wuding catchment. To achieve this aim, a catchment-scale carbon balance was constructed. The major objectives are to: 1) explore the spatial and temporal variability of riverine carbon export, 2) trace the sources and age of the emitted CO_2 using carbon isotope techniques, and 3) evaluate the riverine carbon cycle in relation to the catchment's terrestrial ecosystem production. This study is built upon our earlier work of Ran et al. (2017) in which we analyzed environmental controls and dam impacts on riverine CO_2 emissions. These results will provide insights into riverine carbon studies for rivers in arid-semiarid climates and improve the accuracy of extrapolation from watershed-based carbon studies to global-scale estimates.

2. Study area and methods

2.1 Study area

The Wuding River (37–39° N; 108–110.5° E) is one of the largest tributaries of the Yellow River and located on the central Chinese Loess Plateau (Figure 1). Its drainage area is 30,261 km^2 and multi-annual mean water discharge is 35 m^3 s^{-1}. Based on geomorphological landscape, the catchment can be further divided into the southeastern loess subcatchment covered with 50–100 m deep loess and the northwestern sandy subcatchment composed mainly of aeolian sand (Figure

1). While barren terrain is extensive in the sandy subcatchment, agriculture is the primary land use type in the loess subcatchment with traditional ploughing tillage as the dominant land management practice. Annual precipitation decreases from 500 mm in the southeast to 300 mm in the northwest, of which 75% falls in the wet season from June until September (Li et al., 2007). Several heavy storms in summer can account for half of the annual precipitation. Except the periods of heavy storms, hydrological regime is controlled by groundwater input, especially in the sandy subcatchment. Due to highly erodible loess and sparse vegetation, the Wuding catchment once suffered severe soil erosion of a rate of 7000 t km^{-2} per year (Ran et al., 2017).

Check dams have long been proposed as an effective soil conservation strategy. By 2011, more than 11,000 check dams have been constructed (Ran et al., 2017). Because their primary purpose is for reducing sediment loss, these structures are generally designed without sluice gates. Consequently, most of the sediment from upstream hillslopes and gullies can be effectively trapped (Ran et al., 2013), resulting in a short life time for these dams because of rapid sediment accumulation, generally less than 20 years (Xu et al., 2013). The resulting organic carbon (OC) burial is likely substantial, but remains to be quantified (Zhang et al., 2016), as does the altered CO_2 exchange at the formed standing water surface. Because of widespread presence of calcite in loess (up to 20%; Zhang et al., 1995) and carbonate dissolution and precipitation under dry climate, this catchment shows hard-water attributes in rivers and check dam-formed reservoirs featuring high dissolved solids. Its mean alkalinity was 3850 μmol L^{-1} and long-term river water CO_2 partial pressure (pCO_2) ranged between 1000 and 2500 μatm (Ran et al., 2015a).

2.2 Field sampling and laboratory analysis

While detailed information has been provided in Ran et al. (2017), a brief description was provided here. Three sampling campaigns were conducted in the Wuding catchment in 2015: before the wet season (March–April; denoted as spring), during the wet season (July–August; summer), and after the wet season (September–October; autumn). Sampling was not performed in winter due to ice coverage. The sampling was performed at 74 sites, including 60 river sites in six Strahler order rivers (Strahler, 1957) and 14 reservoir sites in 8 check dam-formed reservoirs (Figure 1). Moreover, monthly samples were collected at the catchment outlet Baijiachuan gauge (Figure 1) in 2017 and daily hydrological records for 2015 and 2017 were also retrieved from the gauge. The sampling frequency was intensified (i.e., 2-h intervals) during typical flood events.

We employed the drifting floating chamber technique to measure *in situ* CO_2 emissions (Ran et al., 2017). Briefly, an infrared Li-7000 gas analyzer (Li-Cor, Inc, USA) was connected to a rectangular chamber (volume: 17.8 L) via rubber-polymer tubes to measure CO_2 concentration changes inside the chamber over time. We also measured *in situ* surface water pCO_2 using the headspace equilibrium method by means of the Li-7000 gas analyzer (Müller et al., 2015). Triple measurements at each site showed a high consistency with 3% variability only. Finally, surface water pCO_2 was calculated and calibrated with the solubility constants for CO_2 from Weiss (1974). To determine the age of the emitted CO_2, we collected radiocarbon ($\Delta^{14}C$) samples by using the precipitation method widely used in groundwater dating studies (Vita-Finzi and Leaney, 2006). After the CO_2 emissions measurement, the accumulated CO_2 in the chamber was directly injected into 50 mL $SrCl_2$ solution in a closed recirculating loop using an external pump.

Biogeosciences Discuss., https://doi.org/10.5194/bg-2018-51
Manuscript under review for journal Biogeosciences
Discussion started: 1 February 2018

Reaction of chamber CO_2 with $SrCl_2$ results in the precipitation of $SrCO_3$. The precipitated $SrCO_3$ was then filtered, dried, and stored in a cool and dark environment until analysis. Eleven $SrCO_3$ samples were collected at four sites during the three campaigns.

Water samples for dissolved organic and inorganic carbon (DOC and DIC) were filtered on site shortly after collection using Whatman filters (0.45 µm pore size). DOC was analyzed on an Elementar Vario TOC select analyzer following procedures in Ran et al. (2017). Total alkalinity was determined by titration in the field and DIC was calculated from total alkalinity, pH, and temperature by using the program CO_2calc (Robbins et al., 2010). We also drilled sediment cores within 4 check dams by using a soil auger (Figure 1). Sediment samples were collected at 20-cm intervals and the drilling depth was 4–6 m depending on sedimentation history. Samples collected from filters and sediment coring for particulate organic carbon (POC) were first dried for 12 h and then pulverized in a mortar. The obtained fine powder was fumigated by concentrated HCl for 24 h to remove inorganic carbon and measured using a PerkinElmer 2400 Series II CHNS/O elemental analyzer (analytical error: <0.3%). Isotopic signature of the eleven $SrCO_3$ samples was determined using accelerator mass spectrometry (AMS) at the Beta Analytic Radiocarbon Dating Laboratory (Miami, USA). The $\Delta^{14}C$ values were reported as percent modern carbon (pMC) based on modern standard and conventional radiocarbon ages were calculated using the ^{14}C half-life (5570 years) following the procedures outlined by Stuiver and Polach (1977). Meanwhile, stable carbon isotope ($\delta^{13}C$) was simultaneously reported and its values were reported in ‰ relative to the VPDB standard at a precision of ±0.3‰ or better.

2.3 Carbon fluxes and CO_2 emissions

Using the monthly sampling results and daily flow and sediment records measured at the catchment outlet Baijiachuan gauge, we calculated the yearly dissolved (DOC and DIC) and particulate (POC) carbon export from the Wuding catchment. This was achieved by multiplying daily flow rates or sediment concentrations averaged over sampling intervals by measured DOC and DIC concentrations in water or POC content in sediments. The yearly total carbon flux was calculated as the sum of the monthly fluxes. Total OC burial behind check dams was estimated by multiplying annual sediment deposition rate by POC content.

Areal fluxes of CO_2 emissions across water-air interface (F_{CO_2}, mmol m^{-2} d^{-1}) was determined from the slope of the linear regression of pCO_2 against time (coefficient of determination r^2 ≥0.97):

$$F_{CO_2} = 1000 \times \left(\frac{dpCO_2}{dt}\right)\left(\frac{V}{RTS}\right) \quad (1)$$

where, $dpCO_2/dt$ is the slope of CO_2 change within the chamber (Pa d^{-1}; converted from µatm min^{-1}), V is the chamber volume, R is the gas constant, T is chamber temperature (K), and S is the area of the chamber covering the water surface (0.09 m^2).

To calculate CO_2 efflux from the entire catchment, we estimated the areal extent of river water surface by means of the 90-m resolution Shuttle Radar Topography Mission (SRTM) DEM data set (Ran et al., 2015b). The delineated drainage network was then classified using the Strahler ordering system (Strahler, 1957). The measured widths of all sampled rivers during fieldwork

were aggregated based on stream order to calculate the water surface area. For reservoirs, our earlier work (Ran and Lu, 2012) has identified their location and areal extent. Both the delineated drainage network and reservoir were calibrated through ground truthing during fieldwork. We further assumed that each round of field sampling was representative of CO_2 emissions for equally four months (i.e., spring sampling: January–April (120 d); summer sampling: May–August (123 d); autumn sampling: September–December (122 d)). With this assumption in mind, we calculated the yearly CO_2 efflux from both rivers and reservoirs.

2.4 Estimation of terrestrial ecosystem production

To evaluate the magnitude of riverine carbon flux, we compared the total carbon entering the drainage network with the Wuding catchment's net ecosystem production (NEP). MOD17A3H (MODIS/Terra Net Primary Production) produced by USGS (https://lpdaac.usgs.gov/) was used to first estimate net primary productivity (NPP). The MOD17A3H Version 6 provides global NPP estimates at 500-m pixel resolution and in units of kg C m^{-2}. While NPP is an important indicator of carbon uptake by terrestrial ecosystems, it does not account for carbon losses through heterotrophic soil respiration (R_h). Heterotrophic soil respiration due to bacterial activities tends to release a significant fraction of the sequestered carbon into the atmosphere, depending on soil temperature, moisture, and substrate availability (Wei et al., 2015). Therefore, the NEP was used for the assessment and it can be estimated by subtracting R_h from NPP:

$$\mathrm{NEP} = \mathrm{NPP} - R_h \quad (2)$$

To calculated R_h, total soil respiration (S_R) was first derived from the global soil CO_2 efflux database described by Raich and Potter (1995) who estimated S_R at a 0.5° latitude by longitude spatial scale. S_R was then divided into its two components of autotrophic and heterotrophic soil respiration. R_h was finally estimated according to the assumption by Hanson et al. (2000) that R_h accounts for 54% and 40% of S_R in forested and non-forested areas, respectively.

3. Results

3.1 Lateral riverine carbon fluxes

DOC concentrations ranged from 1.4 to 9.5 mg L^{-1} throughout the three sampling periods with both the lowest and highest DOC concentrations occurred in spring. The DOC averaged 5, 5.2, and 4.5 mg L^{-1} in spring, summer, and autumn, respectively. DOC first exhibited a downward trend along the river course from headwater downstream and then increased in the 6th order mainstem river in both the sandy and loess subcatchments (Figure 2). While the DOC in the low-order streams (i.e., 1st–2nd) was on average 9.4–20.6% higher than in the 3th–5th order streams, it increased to 5.7 mg L^{-1} in the 6th mainstem. The POC in sediments varied from 0.28% to 1.72% (dry weight) and shown pronounced seasonal variations. The averaged POC content in spring, summer, and autumn was 0.91%, 0.44%, and 0.69%, respectively.

With the pH in range of 7.68–9.29, the calculated DIC was approximately equal to alkalinity. The Wuding waters presented significantly higher DIC than DOC concentrations. DIC in spring, summer, and autumn varied in the range of 39–119, 32–132, and 34–143 mg L^{-1} with the average at 62.1, 66.7, and 67.7 mg L^{-1}, respectively. In the loess subcatchment, the DIC declined remarkably from headwater streams towards the mainstem channel (Figure 3a); but it remained

constant in the sandy subcatchment from the 1st order through the 5th order streams (Figure 3b). The high DIC values in the 6th order mainstem channel in the sandy subcatchment (Figure 3b) is reflective of the confluence of the two subcatchments. If only the 1st–5th order streams were considered, DIC in the sandy subcatchment was 38% lower than that in the loess subcatchment.

At Baijiachuan gauge, the DIC remained highly stable at 39.2±7.8 mg L^{-1} over time. In comparison, the DOC concentration was 16% higher in the wet season than in the dry season while the POC content (range: 0.15–1.16%) in the former was less than half of that in the latter. The mean DOC and POC were 3.3±0.4 mg L^{-1} and 0.61±0.29%, respectively. Because the flow regime in 2017 was significantly biased due to an extreme flood in July (spontaneous discharge: 4490 m^3 s^{-1}; Figure S1 in Supplementary), we used the hydrological data for 2015 to calculate downstream carbon export assuming that carbon content was comparable in 2015 and 2017. The annual downstream carbon export at Baijiachuan gauge was estimated to be $(7\pm1.9)\times10^{10}$ g C, of which the DIC, DOC, and POC fluxes were $(3\pm0.6)\times10^{10}$, $(0.3\pm0.03)\times10^{10}$, and $(3.7\pm1.8)\times10^{10}$ g C, respectively. DOC flux was around 10% of the DIC and POC fluxes, comprising only 4% of the total flux. DIC and POC fluxes were comparable, accounting for 53% and 43%, respectively, of the total flux.

3.2 CO_2 emissions from rivers and check dam-formed reservoirs

In our earlier work, we calculated the areal CO_2 emissions from rivers (Ran et al., 2017). In the sandy subcatchment, the mean CO_2 efflux from the 1st order headwater streams to the 6th order mainstem was 280, 422, 155, 216, 256, and 238 mmol m^{-2} d^{-1}, respectively. In the loess subcatchment, it was 70, 78, 80, 57, 209, 268 mmol m^{-2} d^{-1}, respectively. In association with the water surface area over the three seasons (Table S1 in Supplementary), total CO_2 emissions in 2015 were $(3.7\pm0.5)\times10^{10}$ g C, of which 42% was degassed from the sandy subcatchment rivers and 58% from the loess subcatchment rivers. At the catchment scale, CO_2 outgassing along fluvial transport first decreased from upland headwater rivers until the 4th order rivers, and then increased remarkably in the 5th and 6th order rivers in both subcatchments (Figure 4a). The headwater 1st and 2nd order rivers accounted for 26% of the total CO_2 efflux (Figure 4b). With the biggest areal extent of water-air interface (43% of the total; Table S1 in Supplementary), the 6th order mainstem contributed 54% of the total CO_2 efflux (Figure 4b).

CO_2 effluxes from check dam-formed reservoirs varied from -23.5 to 66.5 mmol m^{-2} d^{-1} in spring, -33.5 to 19 mmol m^{-2} d^{-1} in summer, and -17 to 42.1 mmol m^{-2} d^{-1} in autumn. The mean CO_2 efflux for these three seasons was 4.2, -16.2, and 12.3 mmol m^{-2} d^{-1}, respectively (Ran et al., 2017). Of the 8 reservoirs, 2 reservoirs are located in the sandy subcatchment and 6 in the loess subcatchment (Figure 1). Reservoir CO_2 effluxes in the sandy subcatchment were constantly higher or less negative than that in the loess subcatchment with the mean efflux at 10.4 and -2.9 mmol m^{-2} d^{-1}, respectively. Currently, there are 337 reservoirs in the catchment with the water surface varying from 0.01 to 10.35 km^2 (Figure S2 in Supplementary). Total water surface area is 107 km^2, including 31.8 km^2 in the sandy subcatchment and 75.2 km^2 in the loess subcatchment. Assuming the water surface remained constant (i.e., no significant seasonal fluctuations), the annual CO_2 emissions were conservatively estimated at 38 million mol (or

260 0.05×10^{10} g C; Table 1). CO_2 outgassing in spring and autumn was offset by CO_2 uptake in summer by 85%.

The isotopic composition of the emitted CO_2 varied significantly between sampling sites and between seasons (Table 2). The sandy subcatchment (site S1; Figure 1) showed the most
265 depleted $\delta^{13}C$ signature (-30.2‰). With the $\delta^{13}C$ values most depleted in spring, the mean $\delta^{13}C$ values in spring, summer, and autumn were -30.2‰, -24.5‰, and -23.2‰, respectively. The $\Delta^{14}C$ values also displayed seasonal variations and the conventional age ranged from 810 to 1890 years (Table 2; Figure 5). The emitted CO_2 exhibited the oldest age in spring at all the 4 sites with the age in summer and autumn 36% and 29% younger, respectively. The average ^{14}C age in
270 the three seasons was 1610, 1038, and 1140 years, respectively. There was no discernible correlation between DIC and DOC concentrations and the isotopic composition.

3.3 OC burial behind check dams

Based on our earlier estimate of sediment trapping, the trapping efficiency in this catchment is
275 94.3% and total sediment deposition rate is 3720×10^{10} g year^{-1} (Ran et al., 2013). Analysis of sediment profiles from the four check dams (Figure 1) shows the POC content varied from 0.1% to 0.5% with high POC contents in the surface soils (0–60 cm) and it declined rapidly with depth and remained constant thereafter at around 0.2% (Figure 6). The mean POC content was 0.21±0.11%. Total OC burial behind check dams was estimated to be $(7.8\pm4.1)\times10^{10}$ g C year^{-1}.
280

3.4 Terrestrial NPP and NEP fluxes

The NPP in the Wuding catchment in 2015 was spatially heterogeneous (Figure 7). The mean areal NPP was 221 g C m^{-2} and the total NPP was $(668\pm60)\times10^{10}$ g C. Based on the global soil respiration flux database (Raich and Potter, 1995), the R_h for this catchment is about 450 g C m^{-2}
285 year^{-1}. Recent land use studies show that forest cover in this catchment occupies only 5% of the total area (Wang et al., 2014), while the remaining is dominated by cropland or barren terrain. Using the ratios of autotrophic to heterotrophic soil respiration for forested and non-forested land suggested by Hanson et al. (2000), R_h was estimated to be 183 g C m^{-2} year^{-1} or 554×10^{10} g C year^{-1} in total. By subtracting R_h from NPP, a first-order estimation shows a NEP of 38 g C m^{-2}
290 year^{-1} or 114×10^{10} g C year^{-1} for the entire catchment. The NEP represented only 17% of the NPP, and heterotrophic soil respiration consumed 83% of the sequestered carbon.

4. Discussion

4.1 Carbon export dynamics within the catchment

295 Carbon export from terrestrial ecosystems into drainage networks is controlled by hydrological regime, geomorphological landscape, biogeochemical processes, and human impact within the catchment of concern (Noacco et al., 2017;Stimson et al., 2017). Affected by sparse vegetation coverage, both DOC and POC contents in the Wuding catchment were relatively low compared with most rivers in the world. Stream water OC is susceptible to degradation by microbial or
300 photochemical reactions during transit (Raymond et al., 2016). The downstream DOC decline along the 1st–5th order streams suggests that the labile fraction of DOC was decomposed in the river course (Figure 2). This decomposition is generally associated with increasing water

residence time for bacterial respiration in downstream streams due to decreasing flow velocities. In contrast, the deeply incised headwater streams in the Wuding catchment exhibit an opposite landscape with the flow velocities increasing from headwater streams to the mainstem channel (Ran et al., 2017). Thus, the decreasing water residence time cannot fully explain the decreasing DOC concentration. Instead, the gradually increasing temperature with declining elevation might have enhanced bacterial respiration (Peierls and Paerl, 2010). The water temperature in the lowland streams was on average 2–5 °C higher than in the headwater streams (Ran et al., 2017).

The high DOC values in the 6th mainstem channel reflect direct DOC influxes from low-order streams (Figure 1) and the mixture of carbon export from the two subcatchments. There was no discernible seasonal difference in DOC concentrations in both subcatchments, although the hydrograph varied significantly among the three seasons. Consequently, there was no significant correlation between DOC and flow based on the spatial sampling results ($p>0.05$). Although the extensive implementation of agricultural tillage practices in April and May tends to mobilize vast amounts of OC, OC export through surface runoff into the drainage network is limited to episodic high-discharge events in June to September. The timing inconsistency suggests that the mobilized soil OC in this dry catchment was either leached into deep soil layers or released into the atmosphere after mineralization. Lateral export into the drainage network caused by surface runoff is negligible. The predominance of groundwater input over the entire year and its highly stable DOC illustrates the insensitivity of DOC concentration to flow dynamics. In contrast, the spatial heterogeneity of DIC with higher values in the loess subcatchment was likely caused by dissolution of carbonates which are abundant in loess (Zhang et al., 1995).

The POC content in sediments is at the lower end of global rivers (range: 0.3–10.1%), which reflects the ancient sedimentary OC origin of about 0.5% for fluvial sediments worldwide (Ludwig et al., 1996). This can also be seen from the isotopic signature of the Yellow River sediment that is primarily derived from the Loess Plateau. Wang et al. (2012) found that the exported POC is quite old (4110–8040 years) and biogeochemically refractory. The substantially lower POC contents in summer than in spring and autumn reflected the impact of gully erosion, which is quite common on the Loess Plateau during periods of heavy storms in summer (Wang et al., 2017). Gully erosion is usually associated with the mobilization of subsurface soils that have a substantially lower OC content (i.e., 0.2–0.3%; Ran et al., 2015a) than the surface soils. As a result, input of subsurface soils into rivers caused the lower POC content in summer, thereby generating a negative correlation between POC and suspended solids concentration.

With respect to CO_2 outgassing, the higher effluxes in the drier sandy subcatchment reflect the stronger impact of groundwater input, although both sub-catchments are heavily controlled by groundwater inflow. While several heavy rainstorms in summer are responsible for a large share of the annual precipitation (i.e., >70%; Wang et al., 2017), our field measurements in 2015 did not capture the storm-caused CO_2 outgassing. Thus, the CO_2 emissions results reveal largely the groundwater-derived CO_2 degassing. This may have caused considerable uncertainty in the annual CO_2 outgassing estimation (see discussion below). Although the sandy subcatchment rivers exhibited higher areal CO_2 effluxes than that in the loess subcatchment in all the 1st–5th order rivers except the 6th mainstem, the lower contribution of CO_2 emissions from the former

(42%) is because its water surface accounts for 32% only of the total water surface. In comparison, the larger contribution of the loess subcatchment rivers (58%) reflects their higher drainage density and larger water surface area (68% of the total; Table S1 in Supplementary).

Unlike natural rivers showing strong CO_2 outgassing, the measured reservoirs presented considerably lower and even negative CO_2 effluxes. The contrasting magnitude and direction of CO_2 exchange suggest the physical and biogeochemical differences between lotic and lentic waters. Compared with rivers with fast moving water and high sediment concentrations, reservoirs display greatly reduced flow turbulence and enhanced algal production resulting from inncreased light penetration after the settling of suspended sediment (Cole et al., 2007). Analysis of chlorophyll-*a* also shows that it is 100% higher in reservoirs than in rivers in summer and autumn (Ran et al., 2017), indicative of carbon uptake by aquatic plants through photosynthesis. In the sandy subcatchment, the predominance of groundwater with high pCO_2 has probably maintained its relatively higher reservoir CO_2 effluxes (mean: 10.4 mmol m^{-2} d^{-1}). For the loess subcatchment reservoirs, intensive nutrient loading from agricultural fields may have facilitated the growth of aquatic plants like phytoplankton, causing the net carbon uptake (mean: -2.9 mmol m^{-2} d^{-1}). Overall, these reservoirs differ from their tropical counterparts that typically act as strong CO_2 source hot spots (Barros et al., 2011;Deemer et al., 2016), yet they are consistent with other temperate reservoirs with similar landscape attributes (Knoll et al., 2013). Given the global abundance of hard-water reservoirs and their unique carbon processing mechanisms (Tranvik et al., 2009), estimating global CO_2 emissions from reservoirs must pay comparable attention to these currently underrepresented reservoirs as to their tropical counterparts.

4.2 Downstream carbon export at catchment outlet and OC burial

The monthly carbon export at Baijiachuan gauge illustrates diverse responses of different carbon species to hydrological regime. Hydrologic storm events in wet seasons play a disproportionately important role in transporting terrestrially-derived carbon. Our high-frequency sampling during flooding periods at Baijiachuan gauge indicates that DOC concentrations were ~20% higher in the flooding periods than that in normal flow conditions. The positive correlation between DOC export and hydrography demonstrates the enhanced leaching of organic matter from surface vegetation and organic-rich top soil layers (Hernes et al., 2008). Moreover, increased stream velocities in the flooding periods have reduced water residence time and consequently, even the labile fraction of DOC could be quickly transported downstream, resulting in a greater export of DOC (Raymond et al., 2016). In comparison, the DIC concentration displayed a weak sensitivity to flow dynamics. Widespread presence of calcite in loess and intensive carbonate dissolution tend to provide sufficient DIC input, which have probably prevented the dilution effect observed in many other rivers (Ran et al., 2015a;Raymond and Cole, 2003).

The substantially lower POC content in the wet season largely reflects the impact of gully erosion as discussed earlier. With respect to sediment sources on the Loess Plateau, it has been widely realized that more than 50% of the sediment in wet seasons, especially during heavy storm periods, is derived from subsurface soils through gully erosion (Wang et al., 2017;Ran et al., 2015a). Mobilization of subsurface soils with a low OC content (i.e., 0.2–0.3%) and subsequent fluvial transport resulted in the observed low POC contents in the wet season. Our

results of 0.15–0.26% for samples collected during floods agreed well with the low carbon content in subsurface soils. Despite the low POC content, however, the POC flux in the wet season is considerable on an annual basis because of the high sediment loading.

CO_2 outgassing during flooding periods have also been significantly enhanced due largely to stronger near-surface turbulence and thus a higher gas transfer velocity (Figure 8). The average CO_2 efflux for the monitored flooding period was 5 times that in normal flow conditions (196 vs. 39 mmol m^{-2} d^{-1}). When looking at the annual total fluxes, episodic high-discharge events were responsible for a significant percentage of annual carbon export though the duration of high-discharge events made up 4% only of the sampling year 2017. A conservative calculation using the sampling results at Baijiachuan gauge indicates that 85% of the annual downstream carbon export occurred during the three extreme floods (Figure S1 in Supplementary). Therefore, any sampling strategies missing episodic high-discharge events would create great uncertainties for annual-scale carbon export estimates (Lee et al., 2017;Jung et al., 2014). This is particularly true for arid-semiarid catchments, such as the Wuding River studied here, where episodic rainfall events make an exceptionally large share of annual water and sediment export.

The decreasing POC content in the deposited sediments with depth demonstrates the OC burial efficiency. Soil OC within the Wuding catchment is spatially homogeneous. The content in hillslope soils varies from 0.4–0.7% and it is less than 0.2% in the gully soils due to strong mineralization in the Quaternary loess (Wang et al., 2017), which is approximately equal to the POC content in the trapped sediments. The negligible OC loss after erosion reflects the spatial location and the high sediment trapping efficiency of check dams. Most check dams are located at the bottom of highly erodible loess gullies. This spatial closeness to erosional sites suggests that the eroded soils can be rapidly deposited after a short delivery distance (Wang et al., 2011). In view of the huge sediment deposition by check dams, the resulting OC burial represents an important carbon sink for the atmosphere that would have otherwise been mineralized to form CO_2 or CH_4 along fluvial delivery. It is important to recognize that, as a top priority soil conservation strategy, numerous check dams have been constructed on Loess Plateau over the past 60 years and more are under construction to replace the filled ones (Zhang et al., 2016;Wang et al., 2017). Assessing the potential OC burial efficiency and amount may have important implications for regional and even global carbon budgets. Regional estimates of OC burial in lakes have recently been made (Zhang et al., 2017;Kastowski et al., 2011). Considering the larger number of check dams and reservoirs of China, quantifying their OC burial will be critical for a more robust OC burial assessment in global lakes and reservoirs (Mendonça et al., 2017). Clow et al. (2015) provide a novel attempt to estimate large-scale OC burial by using regression models to extrapolate from limited measurements.

4.3 Carbon isotopic signature in the emitted CO_2

CO_2 emissions from rivers originate from decomposition of organic matter derived from terrestrial ecosystems and/or aquatic photosynthesis. The emitted CO_2 exhibited a ^{13}C-depleted $\delta^{13}C$ signature significantly different from that from carbonate-dominant river basins (i.e., 0‰, Brunet et al., 2009). As stated earlier, the Wuding catchment is characterized by extensive presence of carbonates, and carbonate dissolution is the primary source of DIC to groundwater

(Zhang et al., 1995). Although we did not analyze the $\delta^{13}C$ of DIC, prior studies indicate that it generally ranges from -6.7 to -12.9‰ in Loess Plateau rivers (Liu and Xing, 2012). For natural rivers with the DIC dominated by HCO_3^-, kinetic isotope fractionation due to CO_2 outgassing tends to enrich the $\delta^{13}C$ of DIC by 3–5‰ (Doctor et al., 2008). Therefore, the emitted CO_2 is less likely to be derived from the interactions between water and carbonates, because the kinetic isotope fractionation process is not able to compensate the great discrepancy in $\delta^{13}C$. This is consistent with the $\delta^{13}C$ changes in soil CO_2 in sandy catchments (Gillon et al., 2012).

Instead, the $\delta^{13}C$ values of the emitted CO_2 are close to the isotopic composition of soil organic matter that varies between -24 and -34‰ (Brunet et al., 2009). For the catchment with its runoff in dry seasons dominated by groundwater inputs, the more depleted $\delta^{13}C$ in spring demonstrated the contribution of CO_2 in soil water to CO_2 emissions. In comparison, the $\delta^{13}C$ values were comparatively enriched in summer and autumn (Table 2; Figure 9), which probably suggests the impact of decomposition of C4 plants that have a $\delta^{13}C$ end-member of -12‰ (Brunet et al., 2009). Constrained by dry climate, major crops in the catchment are predominantly C4 plants, such as corn and millet, and their growing season from May until October overlaps well with the summer and autumn samplings. Thus, decomposition of these ^{13}C-enriched organic matter in summer and autumn resulted in more positive ^{13}C than that in spring. In addition, CO_2 diffusion process itself can induce isotopic fractionation (Deirmendjian and Abril, 2018;Geldern et al., 2015). Preferential outgassing of $^{12}CO_2$ may have also contributed to the more depleted $\delta^{13}C$ values in the emitted CO_2 than that of the C4 plants. Aquatic algae with their $\delta^{13}C$ value ranging from -40 to -26‰ (Alin et al., 2008) is likely another contributor, as suggested by the 2-fold higher Chl *a* contents in summer and autumn than in spring at some sites (Ran et al., 2017). Deeply incised stream channels provide favorable stagnant water, albeit highly site-specific, for algae growth during non-flooding periods. However, this process seems to be of minor importance given the low light penetration due to extremely high turbidity.

As a useful tracer, natural radiocarbon has been widely used in terrestrial, aquatic, and marine carbon studies to trace the nature (i.e., age and source) and processing of carbon during transit (Gillon et al., 2012). The $\Delta^{14}C$ exhibited a positive correlation with $\delta^{13}C$, showing an increasing trend from spring through summer to autumn (Figure 9). Because DIC from carbonate dissolution is characterized by typically enriched $\delta^{13}C$ and highly depleted $\Delta^{14}C$ (Mayorga et al., 2005;Brunet et al., 2009), distribution of the sampled CO_2 in this dual-isotope plot also suggests the negligible contribution of carbonate dissolution to CO_2 emissions. Instead, in spring dominated by groundwater influx, aged soil-respired CO_2 and decomposition of old OC leached from deep soil horizons have likely led to the older CO_2 age (Figure 5), which suggests the outgassing of ancient terrestrial OC after entering aquatic systems (McCallister and del Giorgio, 2012). Addition of recently-fixed organic matter in summer and autumn through surface water inputs and decomposition of the labile fraction have played a ‘dilution’ effect, causing the younger age of the emitted CO_2 and thus the seasonal distinctions. Notably, the emitted CO_2 is inconsistent with that from the tropical Amazon rivers where respiration of contemporary young organic matter is the primary source of CO_2 outgassing (Abril et al., 2014;Mayorga et al., 2005). The evasion of old carbon from the Wuding catchment is likely to be widespread in arid-semiarid catchments worldwide with similar hydrological regime and terrestrial ecosystems.

Special efforts are therefore needed to quantify this old CO_2 outgassing and assess its significance for global carbon cycle and climate mitigation over longer timescales than recent sharp anthropogenic CO_2 emissions (i.e., since the 1850s).

4.4 Riverine carbon budget and NEP

Our first-order estimate of NEP for the Wuding catchment indicates that its terrestrial ecosystems sequester only small quantities of carbon on an annual basis. Approximately 83% of the NPP was consumed by microbial activities. This ratio is comparable to the estimate for global temperate semiarid ecosystems (i.e., 84% from Luyssaert et al., 2007) while significantly higher than that for other ecosystems. For example, it is 63% in the tropical Nyong River catchment in western Africa (Brunet et al., 2009) and 42% in the temperate Schwabach River catchment in Germany (Lee et al., 2017). Furthermore, the total carbon export from the Wuding catchment accounted for 16% of its catchment NEP (Figure 10). This percentage of NEP as fluvial export is also substantially higher than recent studies in other regions which found that the sum of DOC, DIC, and CO_2 emissions generally represented <3% of the NEP (e.g., Brunet et al., 2009; Lee et al., 2017). Although POC flux and OC burial are not quantified in these studies, the missing amounts are small due to weak soil erosion and absence of dams in their catchments. Similarly, Shibata et al. (2005) found that the annual export of dissolved and particulate carbon from a first-order catchment in northern Japan made up only 2% of its NEP.

These discrepancies between Wuding and these catchments likely reveal the internal differences in soil property and erosion. Erosion-induced mobilization of heavily weathered soils with high calcite content into the Wuding drainage network exhibit a high DIC concentration and percentage flux (Figure 10). Compared with these catchments with weak soil erosion, the strong soil erosion intensity in the Wuding catchment mobilized huge quantities of carbon into the river network. OC burial through sediment storage plays a significant role in re-distributing the exported carbon (Figure 10). Shibata et al. (2005) did not quantify CO_2 emissions, which can be exceptionally higher than lateral fluxes, especially in first-order streams with strong boundary turbulence (Marx et al., 2017).

While the proportion of total fluvial carbon export to catchment NEP is significantly higher than other catchment-based estimates, this percentage (i.e., 16%) falls into the range of global-scale estimate of 50–70% by Cole et al. (2007). Compared with other ecosystems, the arid-semiarid Wuding catchment has a lower terrestrial NEP but a higher carbon export rate because of severe soil erosion. The resulting 16% likely represents the upper limit of the proportion of fluvial carbon export to terrestrial NEP. Thus, the conservative estimate by Cole et al. (2007) may have overestimated the importance of fluvial export in modulating terrestrial carbon uptake (Lee et al., 2017). Although 16% of the annual NEP was exported into the Wuding drainage network, it is worth noting that ~42% of it was buried behind check dams and sequestered thereafter. Given the rapid sedimentation and subsequent land management (i.e., cropland reclamation), this OC burial could be regarded as a long-term carbon sink (Zhang et al., 2016;Wang et al., 2011;Wang et al., 2017). Carbon loss through CO_2 outgassing can offset only 3% of the catchment NEP (Figure 10). However, this first-order calculation may have underestimated carbon loss because the exported carbon exiting the river mouth is subject to further processing and emission.

From a mass balance point of view, our analysis shows that more carbon was buried in sediments than was emitted as CO_2 from rivers and check dam-formed reservoirs in the Wuding catchment. The 2-fold higher OC burial than CO_2 emissions is partially due to the strong soil erosion and high sediment trapping efficiency of check dams, resulting in high OC burial rates (Mendonça et al., 2017). Another reason is the low drainage density of the river network governed by dry climate, leading to a small extent of water-air interface for CO_2 emissions, though the areal CO_2 emission fluxes are similar in magnitude to rivers in other climate zones (Ran et al., 2017;Wallin et al., 2013). However, it should be noted that this comparison was based only on CO_2 emissions, since CH_4 emissions were not accounted for in the budget, although its contribution is likely negligible owing to high sedimentation rates, low water temperature, and low OC content.

5. Conclusion

The Wuding catchment serves as a typical arid-semiarid study area for assessing the fate of terrestrially-derived riverine carbon. Export of riverine carbon was predominantly composed of DIC due to widespread carbonate dissolution and groundwater input. Export of DOC and DIC displayed pronounced spatial and temporal variability. Continuous mineralization of the labile fraction of DOC has probably caused the spatially downstream decline in DOC concentration in low order streams. Enhanced organic matter inputs from agricultural tillage in spring and from terrestrial ecosystems in summer resulted in higher DOC concentrations. POC content was characterized by strong seasonal variability throughout the catchment or at the catchment outlet, indicating the control of gully erosion in wet seasons in mobilizing subsurface soils with low carbon content. The POC flux is comparable to the DIC flux on an annual basis, both of which are an order of magnitude larger than the DOC flux.

CO_2 emissions represented an important pathway, amounting to 20% of the total riverine carbon flux. Carbon isotopic analysis showed that the age of the emitted CO_2 ranged from 810 to 1890 years. Outgassing of this old carbon previously stored in soils has important biogeochemical implications for carbon budget studies. Our first-order estimate suggests that the riverine carbon export from terrestrial ecosystems was significant when compared with NEP, representing 16% of the latter. Riverine carbon cycle in the Wuding catchment has been greatly modified by check dams through sediment storage. Approximately 42% of the total riverine carbon was buried, roughly twice the carbon loss through CO_2 emissions. With more new check dams under construction, OC burial will be a more vital component in reshaping the carbon balance. In addition, episodic storms play a disproportionate role in annual carbon export and future sampling strategy should attempt to capture these short-duration, high-discharge events to better constrain uncertainty.

Through a comprehensive assessment of riverine carbon in terms of downstream export, OC burial in sediments, and CO_2 emissions in a complete catchment, the present research can be treated as an exploratory study integrating river carbon cycle with terrestrial carbon uptake by ecosystems. A better understanding of linkages between terrestrial ecosystems and fluvial carbon export, and of interactions between environmental controls and human impacts, is essential for providing additional constraints on the accuracy of carbon budget estimates. Moreover, for future

studies of riverine CO_2 emissions, it is critical to trace its isotopic composition and age to more holistically explore its biogeochemical significance.

Acknowledgements: This work was supported by the University of Hong Kong (grant: 104004330), the Natural Science Foundation of China (grants: 91547110 and 41671282), and the National University of Singapore (grant: R-109-000-191-646). The data used are available in Ran et al. (2017) or upon request (Email: ranlishan@gmai.com).

References

Abril, G., Martinez, J.-M., Artigas, L. F., Moreira-Turcq, P., Benedetti, M. F., Vidal, L., Meziane, T., Kim, J.-H., Bernardes, M. C., and Savoye, N.: Amazon River carbon dioxide outgassing fuelled by wetlands, Nature, 505, 395-398, 2014.

Alin, S. R., Aalto, R., Goni, M. A., Richey, J. E., and Dietrich, W. E.: Biogeochemical characterization of carbon sources in the Strickland and Fly rivers, Papua New Guinea, Journal of Geophysical Research: Earth Surface, 113, 2008.

Barros, N., Cole, J. J., Tranvik, L. J., Prairie, Y. T., Bastviken, D., Huszar, V. L., Del Giorgio, P., and Roland, F.: Carbon emission from hydroelectric reservoirs linked to reservoir age and latitude, Nat Geosci, 4, 593-596, 2011.

Battin, T. J., Luyssaert, S., Kaplan, L. A., Aufdenkampe, A. K., Richter, A., and Tranvik, L. J.: The boundless carbon cycle, Nat Geosci, 2, 598-600, 2009.

Brunet, F., Dubois, K., Veizer, J., Nkoue Ndondo, G. R., Ndam Ngoupayou, J. R., Boeglin, J. L., and Probst, J. L.: Terrestrial and fluvial carbon fluxes in a tropical watershed: Nyong basin, Cameroon, Chemical Geology, 265, 563-572, 2009.

Butman, D., and Raymond, P. A.: Significant efflux of carbon dioxide from streams and rivers in the United States, Nat Geosci, 4, 839-842, 2011.

Clow, D. W., Stackpoole, S. M., Verdin, K. L., Butman, D. E., Zhu, Z., Krabbenhoft, D. P., and Striegl, R. G.: Organic carbon burial in lakes and reservoirs of the conterminous United States, Environmental Science & Technology, 49, 7614-7622, 2015.

Cole, J. J., Prairie, Y. T., Caraco, N. F., McDowell, W. H., Tranvik, L. J., Striegl, R. G., Duarte, C. M., Kortelainen, P., Downing, J. A., Middelburg, J. J., and Melack, J.: Plumbing the global carbon cycle: Integrating inland waters into the terrestrial carbon budget, Ecosystems, 10, 171-184, 2007.

Deemer, B. R., Harrison, J. A., Li, S., Beaulieu, J. J., DelSontro, T., Barros, N., Bezerra-Neto, J. F., Powers, S. M., dos Santos, M. A., and Vonk, J. A.: Greenhouse gas emissions from reservoir water surfaces: a new global synthesis, BioScience, 66, 949-964, 2016.

Deirmendjian, L., and Abril, G.: Carbon dioxide degassing at the groundwater-stream-atmosphere interface: isotopic equilibration and hydrological mass balance in a sandy watershed, Journal of Hydrology, doi:10.1016/j.jhydrol.2018.01.003, 2018.

Doctor, D. H., Kendall, C., Sebestyen, S. D., Shanley, J. B., Ohte, N., and Boyer, E. W.: Carbon isotope fractionation of dissolved inorganic carbon (DIC) due to outgassing of carbon dioxide from a headwater stream, Hydrological Processes, 22, 2410-2423, 2008.

Geldern, R., Schulte, P., Mader, M., Baier, A., and Barth, J. A.: Spatial and temporal variations of pCO2, dissolved inorganic carbon and stable isotopes along a temperate karstic watercourse, Hydrological Processes, 29, 3423-3440, 2015.

Gillon, M., Barbecot, F., Gibert, E., Plain, C., Corcho-Alvarado, J. A., and Massault, M.: Controls on ^{13}C and ^{14}C variability in soil CO_2, Geoderma, 189-190, 431-441, 2012.

Hanson, P., Edwards, N., Garten, C. T., and Andrews, J.: Separating root and soil microbial contributions to soil respiration: a review of methods and observations, Biogeochemistry, 48, 115-146, 2000.

Hernes, P. J., Spencer, R. G., Dyda, R. Y., Pellerin, B. A., Bachand, P. A., and Bergamaschi, B. A.: The role of hydrologic regimes on dissolved organic carbon composition in an agricultural watershed, Geochimica et Cosmochimica Acta, 72, 5266-5277, 2008.

Jung, B.-J., Lee, J.-K., Kim, H., and Park, J.-H.: Export, biodegradation, and disinfection byproduct formation of dissolved and particulate organic carbon in a forested headwater stream during extreme rainfall events, Biogeosciences, 11, 6119, 2014.

Kastowski, M., Hinderer, M., and Vecsei, A.: Long-term carbon burial in European lakes: Analysis and estimate, Global Biogeochemical Cycles, 25, 2011.

Knoll, L. B., Vanni, M. J., Renwick, W. H., Dittman, E. K., and Gephart, J. A.: Temperate reservoirs are large carbon sinks and small CO_2 sources: Results from high-resolution carbon budgets, Global Biogeochemical Cycles, 27, 52-64, 2013.

Lee, K. Y., van Geldern, R., and Barth, J. A.: A high-resolution carbon balance in a small temperate catchment: Insights from the Schwabach River, Germany, Appl Geochem, 85, 86-96, 2017.

Li, L.-J., Zhang, L., Wang, H., Wang, J., Yang, J.-W., Jiang, D.-J., Li, J.-Y., and Qin, D.-Y.: Assessing the impact of climate variability and human activities on streamflow from the Wuding River basin in China, Hydrological Processes, 21, 3485-3491, 2007.

Liu, W., and Xing, M.: Isotopic indicators of carbon and nitrogen cycles in river catchments during soil erosion in the arid Loess Plateau of China, Chemical Geology, 296, 66-72, 2012.

Ludwig, W., Probst, J. L., and Kempe, S.: Predicting the oceanic input of organic carbon by continental erosion, Global Biogeochemical Cycles, 10, 23-41, 1996.

Luyssaert, S., Inglima, I., Jung, M., Richardson, A. D., Reichstein, M., Papale, D., Piao, S., Schulze, E., Wingate, L., and Matteucci, G.: CO_2 balance of boreal, temperate, and tropical forests derived from a global database, Global change biology, 13, 2509-2537, 2007.

Marx, A., Dusek, J., Jankovec, J., Sanda, M., Vogel, T., Geldern, R., Hartmann, J., and Barth, J.: A review of CO_2 and associated carbon dynamics in headwater streams: a global perspective, Reviews of Geophysics, 2017.

Mayorga, E., Aufdenkampe, A. K., Masiello, C. A., Krusche, A. V., Hedges, J. I., Quay, P. D., Richey, J. E., and Brown, T. A.: Young organic matter as a source of carbon dioxide outgassing from Amazonian rivers, Nature, 436, 538-541, 2005.

McCallister, S. L., and del Giorgio, P. A.: Evidence for the respiration of ancient terrestrial organic C in northern temperate lakes and streams, Proceedings of the National Academy of Sciences, 109, 16963-16968, 2012.

Mendonça, R., Müller, R. A., Clow, D., Verpoorter, C., Raymond, P., Tranvik, L. J., and Sobek, S.: Organic carbon burial in global lakes and reservoirs, Nature Communications, 8, 1, 2017.

Müller, D., Warneke, T., Rixen, T., Müller, M., Jamahari, S., Denis, N., Mujahid, A., and Notholt, J.: Lateral carbon fluxes and CO_2 outgassing from a tropical peat-draining river, Biogeosciences, 12, 5967-5979, 2015.

Noacco, V., Wagener, T., Worrall, F., Burt, T. P., and Howden, N. J.: Human impact on long-term organic carbon export to rivers, Journal of Geophysical Research: Biogeosciences, 122, 947-965, 2017.

Peierls, B. L., and Paerl, H. W.: Temperature, organic matter, and the control of bacterioplankton in the Neuse River and Pamlico Sound estuarine system, Aquatic Microbial Ecology, 60, 139-149, 2010.

Raich, J. W., and Potter, C. S.: Global patterns of carbon dioxide emissions from soils, Global Biogeochemical Cycles, 9, 23-36, 1995.

Ran, L., and Lu, X. X.: Delineation of reservoirs using remote sensing and their storage estimate: an example of the Yellow River basin, China, Hydrological Processes, 26, 1215-1229, 2012.

Ran, L., Lu., X. X., Xin, Z. B., and Yang, X.: Cumulative sediment trapping by reservoirs in large river basins: A case study of the Yellow River basin, Global and Planetary Change, 100, 308-319, 2013.

Ran, L., Lu, X. X., Richey, J. E., Sun, H., Han, J., Liao, S., and Yi, Q.: Long-term spatial and temporal variation of CO_2 partial pressure in the Yellow River, China, Biogeosciences, 12, 921-932, 2015a.

Ran, L., Lu, X. X., Yang, H., Li, L., Yu, R., Sun, H., and Han, J.: CO_2 outgassing from the Yellow River network and its implications for riverine carbon cycle, Journal of Geophysical Research: Biogeosciences, 120, 1334-1347, 2015b.

Ran, L., Li, L., Tian, M., Yang, X., Yu, R., Zhao, J., Wang, L., and Lu, X. X.: Riverine CO_2 emissions in the Wuding River catchment on the Loess Plateau: Environmental controls and dam impoundment impact, Journal of Geophysical Research: Biogeosciences, 122, 1439-1455, 2017.

Raymond, P. A., and Cole, J. J.: Increase in the export of alkalinity from North America's largest river, Science, 301, 88-91, 2003.

Raymond, P. A., Hartmann, J., Lauerwald, R., Sobek, S., McDonald, C., Hoover, M., Butman, D., Striegl, R., Mayorga, E., and Humborg, C.: Global carbon dioxide emissions from inland waters, Nature, 503, 355-359, 2013.

Raymond, P. A., Saiers, J. E., and Sobczak, W. V.: Hydrological and biogeochemical controls on watershed dissolved organic matter transport: pulse-shunt concept, Ecology, 97, 5-16, 2016.

Regnier, P., Friedlingstein, P., Ciais, P., Mackenzie, F. T., Gruber, N., Janssens, I. A., Laruelle, G. G., Lauerwald, R., Luyssaert, S., and Andersson, A. J.: Anthropogenic perturbation of the carbon fluxes from land to ocean, Nat Geosci, 6, 597-607, 2013.

Richey, J. E., Melack, J. M., Aufdenkampe, A. K., Ballester, V. M., and Hess, L. L.: Outgassing from Amazonian rivers and wetlands as a large tropical source of atmospheric CO_2, Nature, 416, 617-620, 2002.

Robbins, L., Hansen, M., Kleypas, J., and Meylan, S.: CO_2calc: A user-friendly seawater carbon calculator for Windows, Mac OS X, and iOS (iPhone), US Geological Survey Open File Report 2010-1280, 2010.

Shibata, H., Hiura, T., Tanaka, Y., Takagi, K., and Koike, T.: Carbon cycling and budget in a forested basin of southwestern Hokkaido, northern Japan, Ecol Res, 20, 325-331, 2005.

Stimson, A., Allott, T., Boult, S., and Evans, M.: Fluvial organic carbon composition and concentration variability within a peatland catchment–implications for carbon cycling and water treatment, Hydrological Processes, 31, 4183–4194, 2017.

Strahler, A. N.: Quantitative analysis of watershed geomorphology, Eos, Transactions American Geophysical Union, 38, 913-920, 1957.

Stuiver, M., and Polach, H. A.: Discussion reporting of ^{14}C data, Radiocarbon, 19, 355-363, 1977.

Tranvik, L. J., Downing, J. A., Cotner, J. B., Loiselle, S. A., Striegl, R. G., Ballatore, T. J., Dillon, P., Finlay, K., Fortino, K., Knoll, L. B., Kortelainen, P. L., Kutser, T., Larsen, S., Laurion, I., Leech, D. M., McCallister, S. L., McKnight, D. M., Melack, J. M., Overholt, E., Porter, J. A., Prairie, Y., Renwick, W. H., Roland, F., Sherman, B. S., Schindler, D. W., Sobek, S., Tremblay, A., Vanni, M. J., Verschoor, A. M., von Wachenfeldt, E., and Weyhenmeyer, G. A.: Lakes and reservoirs as regulators of carbon cycling and climate, Limnology and Oceanography, 54, 2298-2314, 2009.

Vita-Finzi, C., and Leaney, F.: The direct absorption method of ^{14}C assay—historical perspective and future potential, Quaternary Science Reviews, 25, 1073-1079, 2006.

Wallin, M. B., Grabs, T., Buffam, I., Laudon, H., Ågren, A., Öquist, M. G., and Bishop, K.: Evasion of CO_2 from streams–The dominant component of the carbon export through the aquatic conduit in a boreal landscape, Global Change Biology, 19, 785-797, 2013.

Wang, J., Cheng, F., Wang, Y., Chen, H., and Yu, Q.: Spatial-temporal changes of land use in Wuding River Basin under ecological restoration, Bulletin of Soil and Water Conservation, 34, 237-243 (in Chinese), 2014.

Wang, X., Ma, H., Li, R., Song, Z., and Wu, J.: Seasonal fluxes and source variation of organic carbon transported by two major Chinese Rivers: The Yellow River and Changjiang (Yangtze) River, Global Biogeochemical Cycles, 26, GB2025, doi:10.1029/2011gb004130, 2012.

Wang, Y., Fu, B., Chen, L., Lü, Y., and Gao, Y.: Check dam in the Loess Plateau of China: engineering for environmental services and food security, Environmental Science & Technology, 45, 10298-10299, 2011.

Wang, Y., Fang, N., Tong, L., and Shi, Z.: Source identification and budget evaluation of eroded organic carbon in an intensive agricultural catchment, Agriculture, Ecosystems & Environment, 247, 290-297, 2017.

Wei, H., Chen, X., Xiao, G., Guenet, B., Vicca, S., and Shen, W.: Are variations in heterotrophic soil respiration related to changes in substrate availability and microbial biomass carbon in the subtropical forests?, Scientific reports, 5, 2015.

Weiss, R. F.: Carbon dioxide in water and seawater: the solubility of a non-ideal gas, Marine Chemistry, 2, 203-215, 1974.

Xu, Y., Fu, B., and He, C.: Assessing the hydrological effect of the check dams in the Loess Plateau, China, by model simulations, Hydrol Earth Syst Sc, 17, 2185-2193, 2013.

Zhang, F., Yao, S., Xue, B., Lu, X., and Gui, Z.: Organic carbon burial in Chinese lakes over the past 150 years, Quaternary International, 438, 94-103, 2017.

Zhang, H., Liu, S., Yuan, W., Dong, W., Xia, J., Cao, Y., and Jia, Y.: Loess Plateau check dams can potentially sequester eroded soil organic carbon, Journal of Geophysical Research: Biogeosciences, 121, 1449-1455, 2016.

Zhang, J., Huang, W. W., Létolle, R., and Jusserand, C.: Major element chemistry of the Huanghe (Yellow River), China: Weathering processes and chemical fluxes, Journal of Hydrology, 168, 173-203, 1995.

Biogeosciences Discuss., https://doi.org/10.5194/bg-2018-51
Manuscript under review for journal Biogeosciences
Discussion started: 1 February 2018

Table 1. CO_2 emissions from check dam-formed reservoirs within the Wuding catchment.

Subcatchment	Spring	Summer	Autumn	Spring (120 d)	Summer (123 d)	Autumn (122 d)
	mmol m^{-2} d^{-1}			million mol		
Sandy subcatchment	28±36.2	-12±19.3	15.3±5.6	107±138	-47±75	59±22
Loess subcatchment	-2.9±9.9	-17.4±14.8	11.5±17.6	-26±89	-161±137	106±161
Total				81±165	-208±156	165±163

Table 2. Carbon isotope signature of the emitted CO_2 from the Wuding catchment.

Site	Spring			Summer			Autumn		
	pMC	Age (year)	$\delta^{13}C$ (‰)	pMC	Age (year)	$\delta^{13}C$ (‰)	pMC	Age (year)	$\delta^{13}C$ (‰)
S1	82.3±0.3	1560	-32.3	88±0.3	1030	-33.9	84.2±0.3	1380	-24.4
S2	79±0.3	1890	-27.5	84±0.3	1400	-22.2	86±0.3	1220	-19.9
S3	85.1±0.3	1290	-26.5	90.4±0.3	810	-22.7	90.3±0.3	820	-25.2
S4*	80.9±0.3	1700	-34.3	89.3±0.3	910	-19.3			

*Sample for site S4 in October was lost during treatment.

Biogeosciences Discuss., https://doi.org/10.5194/bg-2018-51
Manuscript under review for journal Biogeosciences
Discussion started: 1 February 2018

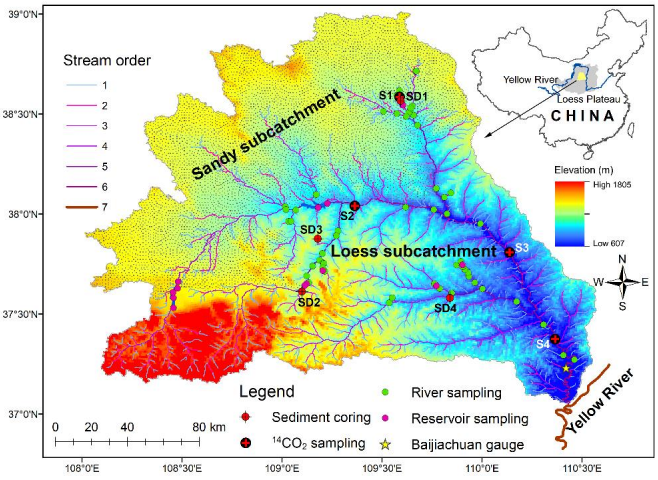

Figure 1. Map of the Wuding catchment showing the sampling sites. SD1–SD4 and S1–S4 denote the sampling location of sediment coring behind check dams and carbon isotope, respectively.

750

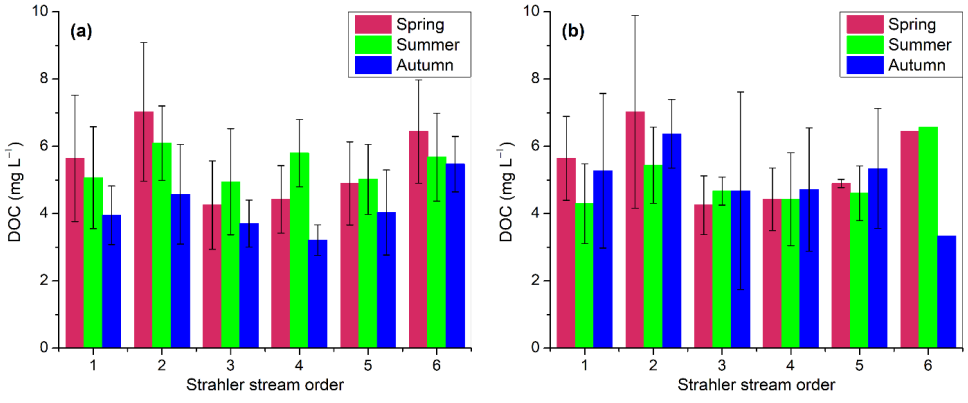

Figure 2. Spatial changes in DOC along the 6 Strahler stream orders in (a) loess subcatchment and (b) sandy subcatchment. Error bars denote the standard deviation.

Biogeosciences Discuss., https://doi.org/10.5194/bg-2018-51
Manuscript under review for journal Biogeosciences
Discussion started: 1 February 2018

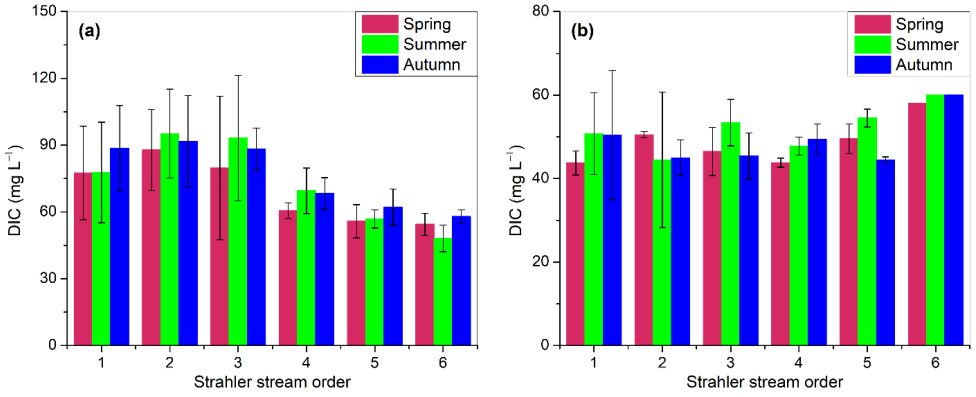

Figure 3. Spatial changes in DIC along the 6 Strahler order streams in (a) loess subcatchment and (b) sandy subcatchment. Error bars denote the standard deviation.

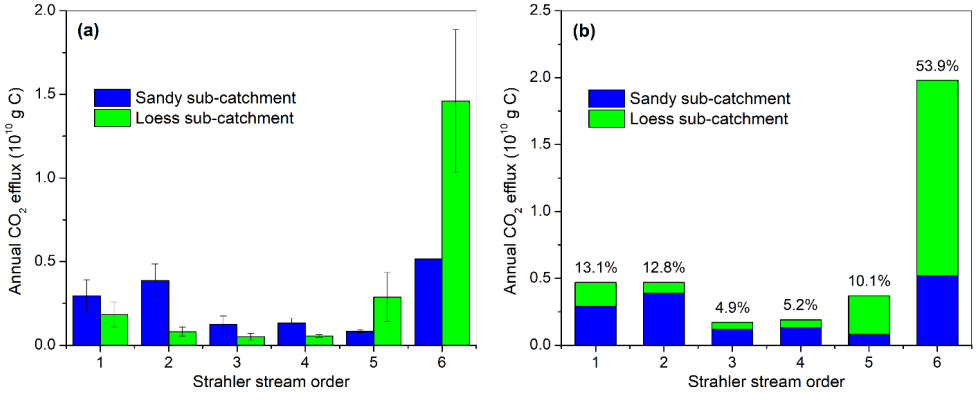

Figure 4. Longitudinal changes in CO_2 emissions along stream order in (a) the sandy subcatchment and the loess subcatchment and (b) the entire Wuding catchment (b). Error bars denote the standard deviation.

Biogeosciences Discuss., https://doi.org/10.5194/bg-2018-51
Manuscript under review for journal Biogeosciences
Discussion started: 1 February 2018

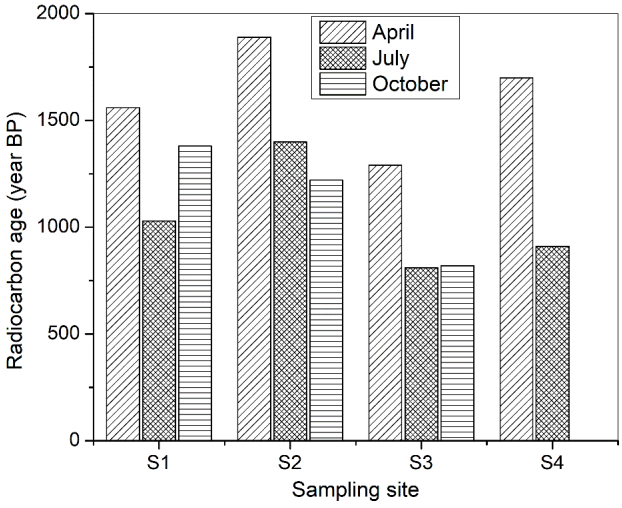

Figure 5. Seasonal variations in conventional age of the emitted CO_2 from the Wuding catchment.

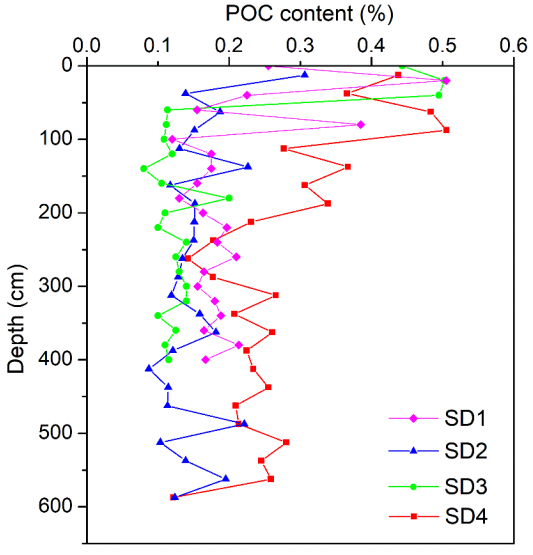

765 Figure 6. Variations of POC content with depth in buried sediments behind check dams (refer to Figure 1 for their location).

Biogeosciences Discuss., https://doi.org/10.5194/bg-2018-51
Manuscript under review for journal Biogeosciences
Discussion started: 1 February 2018

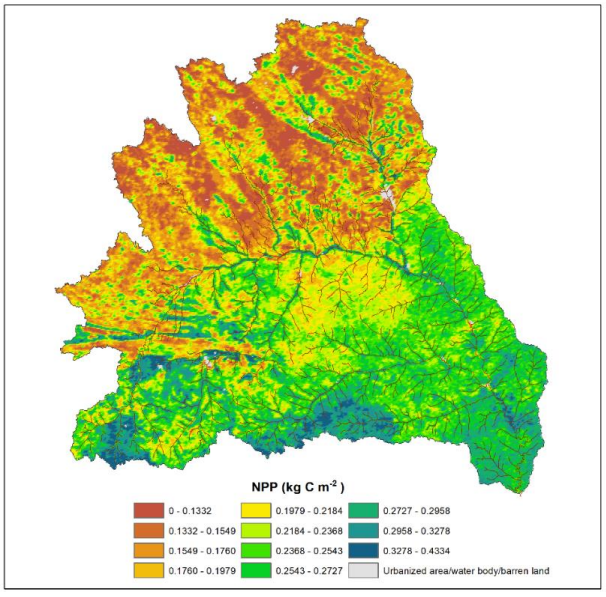

Figure 7. Spatial distribution of NPP within the Wuding catchment in 2015 showing significant differences between the sandy and loess subcatchments.

770

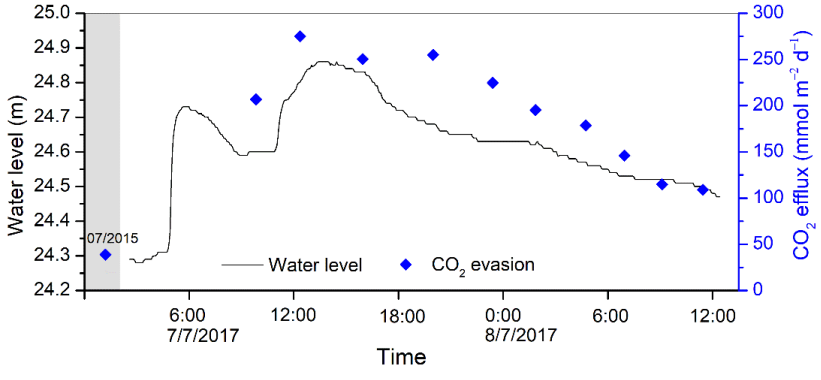

Figure 8. Temporal variation in CO_2 efflux during a high-discharge flood event in the Wuding River at Baijiachuan gauge (refer to Figure 1 for its location).

Biogeosciences Discuss., https://doi.org/10.5194/bg-2018-51
Manuscript under review for journal Biogeosciences
Discussion started: 1 February 2018

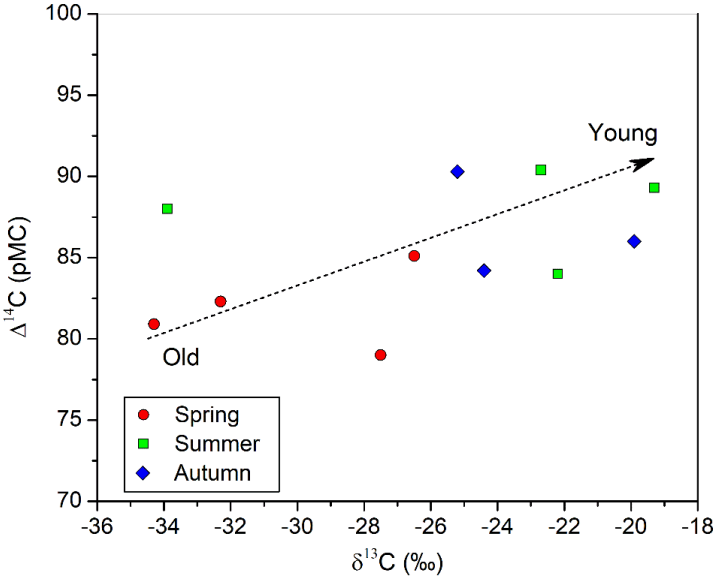

Figure 9. Relationship between $\delta^{13}C$ and $\Delta^{14}C$ of the emitted CO_2 from the Wuding catchment.

775

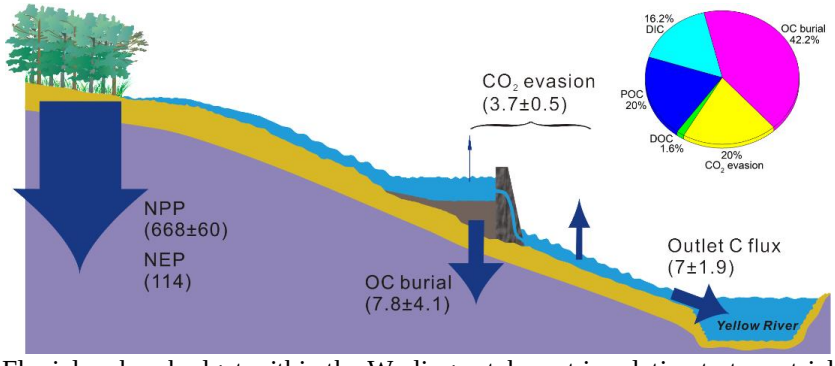

Figure 10. Fluvial carbon budget within the Wuding catchment in relation to terrestrial ecosystem production (unit: $\times 10^{10}$ g C yr^{-1}). The inserted pie chart denotes the partitioning of
780 fluvial carbon among its five phases.